A manganese transporter, BB0219 (BmtA), is required for virulence by the Lyme disease spirochete, *Borrelia burgdorferi*

Zhiming Ouyang[a], Ming He[b], Tara Oman[b], X. Frank Yang[b], and Michael V. Norgard[a,1]

[a]Department of Microbiology, University of Texas Southwestern Medical Center, Dallas, TX 75390; and [b]Department of Microbiology and Immunology, Indiana University School of Medicine, Indianapolis, IN 46202

Communicated by Jonathan W. Uhr, University of Texas Southwestern Medical Center, Dallas, TX, December 19, 2008 (received for review December 4, 2008)

***Borrelia burgdorferi* (*Bb*), the causative agent of Lyme disease, is transmitted to mammalian hosts through an arthropod (tick) vector. To establish infection, *Bb* must acquire essential nutrients, including transition metals, from its mammalian and tick hosts. Thus far, no metal transporter has been identified in *Bb*. Here, we report the identification of the first metal transporter, BmtA (BB0219), in *Bb*. BmtA-deficient mutants of virulent *Bb* were readily generated, and the mutants grew slightly slower than wild-type *Bb* in vitro. However, BmtA mutants were sensitive to the chelating actions of EDTA, suggesting a role for BmtA in metal utilization. Intracellular accumulation of manganese (Mn) was substantially diminished in the *bmtA* mutant, indicating that BmtA was operative in Mn uptake. Given that BmtA lacks homology to any known Mn transporter, we postulate that BmtA is part of a novel mechanism for Mn acquisition by a bacterial pathogen. BmtA also was essential to the infectious life cycle of *Bb* in ticks and mammals, thereby qualifying BmtA as a new borrelial virulence factor. In addition, the *bmtA* mutant was sensitive to treatment with *t*-butyl hydroperoxide, implying that BmtA, and thus Mn, is important to *Bb* for detoxifying reactive oxygen species, including those potentially liberated by immune effector cells during the innate immune response. Our discovery of the first molecule involved in metal transport in *Bb* provides a foundation for further elucidating metal homeostasis in this important human pathogen, which may lead to new strategies for thwarting Lyme disease.**

metal transport | pathogenesis

Lyme disease, caused by the spirochetal bacterium *Borrelia burgdorferi* (*Bb*), remains the most common vector-borne disease in the United States (1). *Bb* has a complex life cycle involving an arthropod (*Ixodes scapularis* tick) vector and various mammalian hosts (2, 3). In recent years, extensive efforts have been directed toward elucidating the mechanisms by which *Bb* cycles, adapts, and sustains itself in these diverse niches. It is now well established that outer surface (lipo)protein C (OspC), OspA/B, decorin-binding protein B/A (DbpB/A), PncA, and BptA are required by *Bb* for efficient infection of ticks or mammalian hosts (4–10). It is also generally accepted that the recently discovered Rrp2-RpoN (σ^{54})-RpoS (σ^{S}) regulatory pathway plays prominently in *Bb*'s virulence expression (11–14).

Transition metals, including iron (Fe), zinc (Zn), and manganese (Mn), are critical to both bacterial metabolism and virulence (15–18). However, transition metals are tightly sequestered within mammalian body fluids, making the scavenging of these cofactors by bacteria challenging. To overcome this, bacteria have evolved a number of elegant systems for acquiring transition metals from their environments. For example, *Escherichia coli* possesses multiple iron uptake systems (18, 19), the MntH Mn transporter (17, 20), and 2 Zn transporters (ZnuABC and ZupT) (16, 21). By tight regulation of these systems, bacteria maintain metal homeostasis.

Compared with other bacterial pathogens, little is known about transition metal acquisition and homeostasis in *Bb*. Genome sequence analysis has implied that *Bb* lacks genes encoding Fe-acquisition systems (22), suggesting unconventionally that Fe may not be required by this pathogen. This assertion was corroborated by an elegant study showing that *Bb* accumulates Mn, rather than Fe, when grown in a serum-free medium (23). However, evidence has been lacking regarding whether *Bb* requires Mn for growth and proliferation and, more importantly, to what extent Mn is needed by *Bb* to establish mammalian infection and how *Bb* acquires this element.

Blast analysis of the *Bb* genome has not revealed obvious homologs of known Mn transporters. However, the *Bb* chromosomal gene *bb0219* encodes a GufA homolog with unknown function (22). Upon comprehensive sequence analysis, we discovered that BB0219 possesses the signature sequence (Axxx**H**-NxxxGLAVG) for the ZIP family [zinc-regulated metal transporters (ZRTs) and iron-regulated metal transporters(IRTs)-like protein family] (24), whose members typically are competent for the uptake of Zn, Fe, or Mn (16, 21, 25, 26). Thus, we postulated that *bb0219* may be involved in the uptake of one or more transition metals by *Bb*. To examine this possibility, we generated isogenic *bb0219* mutants and complemented strains of virulent *Bb* and examined their phenotypes with respect to metal accumulation and their abilities to infect ticks and mice.

Results

In Silico Analysis of BB0219, a GufA Homolog. Blast searches revealed that, in addition to *Bb*, functionally uncharacterized homologs of BB0219 exist in other bacteria, such as *Borrelia garinii*, *Borrelia afzelii*, *Clostridium botulinum*, *Methanococcus maripaludis*, *Desulfotalea psychrophila*, *Staphylococcus epidermidis*, and *Listeria monocytogenes*. Originally, *bb0219* was annotated as GufA, a protein with unknown function (22, 27). GufA proteins have been placed as a subgroup of the larger ZIP family (25). In bacteria, some ZIP proteins transport not only Zn^{2+}, but also other cations, such as Mn^{2+}, Fe^{2+}, and Cd^{2+} (16, 21, 25). All functionally characterized ZIP proteins contain a conserved topology with 8 transmembrane domains. This topology also was predicted to be in BB0219 when we analyzed BB0219 by using protein topology prediction programs PSORTb (28) and TMHMM 2.0 (26). Most ZIP proteins contain a metal-binding site (HxHxH) between spanners III and IV (24), and all ZIP proteins

Author contributions: Z.O. and M.V.N. designed research; Z.O., M.H., T.O., and X.F.Y. performed research; Z.O., M.H., T.O., and X.F.Y. analyzed data; and Z.O. and M.V.N. wrote the paper.

The authors declare no conflict of interest.

[1]To whom correspondence should be addressed. E-mail: michael.norgard@utsouthwestern.edu.

This article contains supporting information online at www.pnas.org/cgi/content/full/0812999106/DCSupplemental.

© 2009 by The National Academy of Sciences of the USA

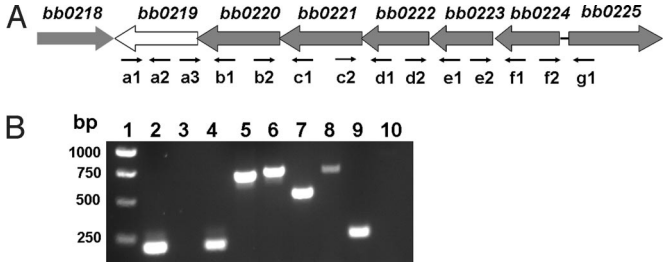

Fig. 1. *bb0219* is cotranscribed with *bb0220–bb0224*. (*A*) Schematic representation of the putative *bb0219–bb0224* operon in *Bb*. (*B*) Results from RT-PCR. Lane 1, molecular weight markers; lane 2, primer pair a1 and a2 in ordinary PCR using genomic DNA as template; lane 3, primer pair a1 and a2 in ordinary PCR using RNA as template (no RT control); lane 4, primer pair a1 and a2; lane 5, primer pair a3 and b1; lane 6, primer pair b2 and c1; lane 7, primer pair c2 and d1; lane 8, primer pair d2 and e1; lane 9, primer pair e2 and f1; and lane 10, primer pair f2 and g1.

have a signature sequence (AxxxHNxxxGLAVG) in the most conserved spanner IV (of which the conserved central histidine provides an intramembranous heavy metal ion-binding site) (24). When we analyzed BB0219, we noted that although the metal-binding motif HxHxH was not apparent, the predicted protein possesses the signature sequence (AxxxHNxxxGLAVG) for the ZIP family (24) in the putative spanner IV region. These in silico analyses thus implicated BB0219 in metal uptake by *Bb*.

***bb0219* Is Cotranscribed Within a 6-Gene Operon.** In the *Bb* genome, *bb0219*, *bb0220*, *bb0221*, *bb0222*, *bb0223*, and *bb0224* are oriented in the same direction (Fig. 1*A*). In this region, *bb0219* is separated from *bb0220* by 40 bp, *bb0223* is separated from *bb0222* by 20 bp, and no intergenic regions are predicted between the other adjacent genes (22). To determine whether these genes are cotranscribed, RT-PCR was performed on RNA by using specific primers [supporting information (SI) *Methods* and Table S1]. As shown in Fig. 1*B* (lane 5), a fragment was amplified by using the primer pair spanning the junction of *bb0219* and *bb0220*. Similar results were obtained for primer pairs spanning the junctions of *bb0221* and *bb0220* (lane 6), *bb0222* and *bb0221* (lane 7), *bb0223* and *bb0222* (lane 8), and *bb0224* and *bb0223* (lane 9), but not in the amplification using primers spanning *bb0225* and *bb0224* (lane 10). Results from all positive and negative controls were as expected (Fig. 1*B*, lanes 2–4). These data indicate that *bb0219–bb0224* are cotranscribed.

Inactivation and Complementation of *bb0219* in *Bb*. *bb0219* disruption mutants were constructed via homologous recombination (Fig. 2*A*). Through allelic exchange, a 740-bp internal fragment of the 822-bp ORF of *bb0219* was replaced with the P*flgB*-kan cassette, yielding 2 kanamycin-resistant transformants, OY04/D4 and OY04/F42. To complement the *bb0219* mutants, the shuttle vector pOY15 was created by fusing *bb0219* to the *Bb flaB* promoter P*flaB* (Fig. 2*A*). After electroporation of pOY15 into OY04/D4 or OY04/F42, 2 corresponding complemented clones, OY06/D11 and OY06/F6, were created. In addition, 2 mock-complemented strains, OY07/F1 and OY07/F62, also were generated by transforming the empty shuttle vector pJD54 into OY04/D4 or OY04/F42, respectively. The inactivation and complementation of *bb0219* in these strains were confirmed by using PCR amplification (Fig. 2*B*), and the insertion and orientation of the P*flgB*-kan cassette within the disrupted *bb0219* gene were confirmed by sequence analysis. Complementation also was confirmed by recovery of the shuttle vector from the complemented strains.

To assess the expression of *bb0219* in *Bb* strains, RT-PCR employing specific primers was performed to detect transcripts.

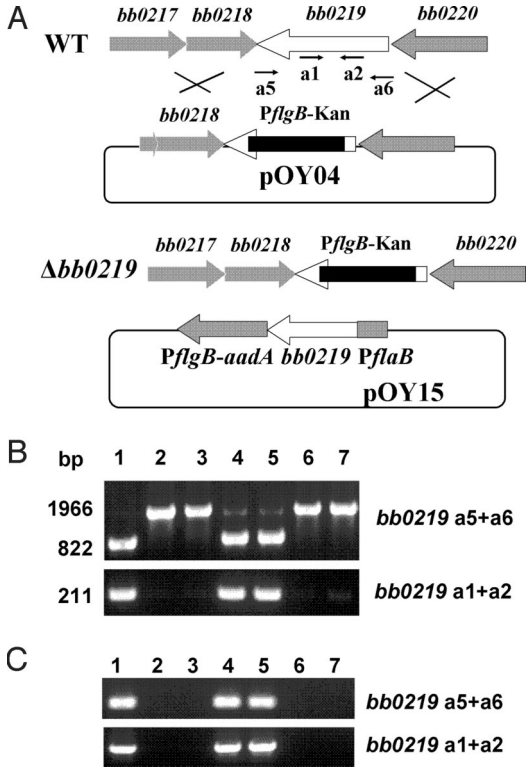

Fig. 2. Construction of *bb0219* disruption mutants and complemented strains. (*A*) Schematic representation of *bb0217–bb0220* genes in the *Bb* chromosome, insertion of the P*flgB*-kan gene cassette by homologous recombination, and the relevant complementation plasmid. Arrows indicate the approximate positions of the oligonucleotide primers used for subsequent PCR analyses. (*B*) PCR analysis of WT 297, *bb0219* mutants, and the complemented strains. The *bb0219*-specific primer pairs used in PCR are indicated on the right. Lane 1, WT 297; lane 2, *bb0219* mutant OY04/D4; lane 3, mutant OY04/F42; lane 4, complemented strain OY06/D11; lane 5, complemented strain OY06/F6; lane 6, mock-complemented strain OY07/F1; and lane 7, mock-complemented OY07/F62. (*C*) RT-PCR was used to determine the presence or absence of *bb0219* transcripts. Lanes and primer pair designations are as in *B*.

As expected, *bb0219* transcripts were detected in both WT 297 and the complemented strains, but not in the mutants and the mock-complemented clones (Fig. 2*C*). *Borrelia* plasmids, especially those that are virulence-associated (such as lp25 and lp28–1), are easily lost during in vitro genetic manipulation, culminating in a loss of borrelial virulence (29). Hence, PCR-based plasmid profiling was performed to ensure that all plasmids were retained in the mutant and complemented strains. As shown in Fig. S1, the *bb0219* mutant OY04/D4 contained the same plasmid profile as that of WT 297. In addition, the *bb0219* mutant clone OY04/F42, the complemented strains (OY06/D11 and OY06/F6), and the mock-complemented strains (OY07/F1 and OY07/F62) also contained all plasmids present in WT 297.

Involvement of BB0219 in Metal Uptake. Under darkfield microscopy, the *bb0219* mutant exhibited spirochetal morphology identical to that of the 297 parental strain. Mutant spirochetes grew slightly slower than wild type in Barbour-Stoenner-Kelly II (BSK-II) medium (approximately a 3.6-fold difference in spirochete numbers between the WT and mutant after 9 days; Fig. S2). When the *bb0219* mutation was complemented by using pOY15, spirochetal growth was restored to the same level as WT 297. To determine whether the mutant had a defect in growth in a mammalian environment, borreliae were cultivated in dialysis membrane chambers (DMCs) implanted into the peritoneal

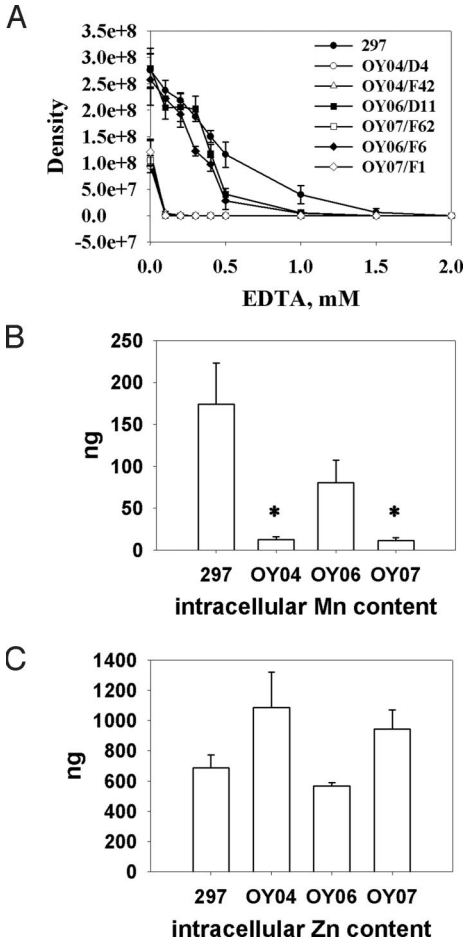

Fig. 3. Role of metals in spirochete growth. In all experiments, BSK-II medium was inoculated with 1,000 spirochetes per mL. After growth at 37 °C for 9 days, spirochetes were collected and enumerated by darkfield microscopy. Data were derived from 3 independent experiments. Error bars indicate standard deviations, and the asterisk indicates statistical significance using Student's *t* test ($P < 0.05$). (*A*) Metal ions were depleted from BSK-II medium by adding varying amounts of EDTA; bacterial growth under these conditions was monitored. (*B* and *C*) Spirochetes from 200 mL of culture were collected, and the intracellular Mn (*B*) and Zn (*C*) contents were measured by inductively coupled plasma atomic emission spectrometry. Values are shown as nanograms per 2.5×10^{10} spirochetes of strains WT 297, *bb0219* mutant OY04/D4, complemented strain OY06/D11, or mock-complemented strain OY07/F62. For Mn contents in OY04 and OY07, the detection limit (10 ng per 2.5×10^{10} spirochetes) is represented, as values were below this threshold.

cavities of rats. After 12 days in DMCs, spirochetes of *Bb* strains 297, the *bb0219* mutant, and the complemented strain increased comparably from 10^3/mL to $\approx 10^7$/mL. These combined findings suggest that *bb0219* is not essential for *Bb* growth either in vitro or in a surrogate mammalian model system.

Because *bb0219* was postulated to encode a metal transporter, we first examined the response of *Bb* to metal limitation by comparing the growth of WT 297, *bb0219* mutants, and complemented strains under metal-restricted conditions. As shown in Fig. 3*A*, the growth of the *bb0219* mutants (OY04/D4 and OY04/F42) was inhibited when bacteria were cultivated in the presence of EDTA. Growth of the *bb0219* mutants was completely inhibited in the presence of 0.1 mM EDTA, whereas WT 297 and the complemented strains (OY06/F6 and OY06/D11) grew well under this condition. This metal-associated phenotype implies that BB0219 is related to metal acquisition by *Bb*, prompting us to rename *bb0219* as *bmtA* for *Borrelia* metal transport protein A.

To garner more direct evidence for the involvement of BmtA in metal transport, we measured the intracellular metal content of various *Bb* strains. We hypothesized that if BmtA indeed is a metal transporter, the accumulation of one or more metals that BmtA transports would be impaired in BmtA-deficient mutants. To assess this, borreliae grown in BSK-II medium were harvested and lysed, and the metal contents within the hydrolysates were determined. We found 174 or 81 ng of Mn in 2.5×10^{10} spirochetes of the WT or complemented strain, respectively (Fig. 3*B*). In contrast, Mn was not detected (below the detection limit of 10 ng) in the same numbers of spirochetes of the *bmtA* mutant or the mock-complemented strain. Because in silico analyses indicated that BmtA might be a Zn-transporting ZIP protein, we also compared the Zn contents among these isolates. Contrary to our expectations, intracellular Zn accumulation was not reduced in the BmtA-deficient mutants (Fig. 3*C*). In fact, the BmtA-deficient mutants appeared to accumulate more Zn than the WT or the complemented strains (Fig. 3*C*). The BmtA-deficient mutants also accumulated magnesium (Mg) at levels comparable to those of WT 297. The combined data indicate that *bmtA* encodes a protein involved in Mn transport, rather than in Zn or Mg transport, in *Bb*.

We also investigated *Bb*'s sensitivity to Mn as a surrogate marker of Mn uptake. When spirochetes were grown in BSK-II medium containing exogenously added Mn, WT 297 was substantially more sensitive to Mn toxicity (60% growth inhibition at 50 μM Mn) than the BmtA-deficient mutant (no growth inhibition at 50 μM Mn), as we predicted (Fig. S3). These data were consistent with the conclusion that BmtA is involved in the uptake of Mn by *Bb*.

BmtA Is Essential for *Bb* to Establish Mammalian Infection. To investigate the contribution of *bmtA* to *Bb* mammalian infectivity, C3H/HeN mice were infected intradermally with various *Bb* strains. After 4 weeks, skin, heart, and joint tissues were collected and transferred into fresh BSK-II medium. Cultures were monitored for 4 weeks for spirochete growth. Whereas motile spirochetes were recovered from tissues of all mice inoculated with 10^4 spirochetes of either the WT or complemented strains (OY06/F6 and OY06/D11), no bacterial growth was observed in any cultures of tissues from mice infected with either 10^4 or 10^7 of the *bmtA* mutants (OY04/D4 and OY04/F42) or mock-complemented strains (OY07/F1 and OY07/F62) (Table 1). These results demonstrate that *bmtA* is essential for mammalian infectivity by *Bb*.

***BmtA* Is Required by *Bb* to Infect Ticks.** Because the *bmtA* mutant was unable to infect mice, it was not possible to examine the contribution of BmtA to the entire *Bb* infectious cycle between ticks and mammals (mice). Therefore, as an alternative means to assess the ability of the *bmtA* mutant to infect, multiply, and survive in ticks, we used a microinjection technique to introduce spirochetes into sterile nymphs. Microinjected ticks carrying various *Bb* strains then were allowed to feed on naïve mice, and naturally detached ticks were collected and dissected, and tick tissue contents were subjected to immunofluorescence assays. As shown in Fig. 4, in contrast to WT 297 and the complemented strain (OY06), the *bmtA* mutant (OY04) was unable to colonize and survive in ticks. Comparable results also were obtained when larval ticks were alternatively infected by using a tick immersion method (30). The combined data demonstrated that *bmtA* is required by *Bb* to infect and survive in its arthropod vector.

BmtA Is Important for Protecting *Bb* Against Reactive Oxygen Species (ROS). In many bacteria, Fe is involved in antioxidant activities, primarily through the ability of Fe^{2+} to reduce H_2O_2 and by functioning as a key cofactor of superoxide dismutase (SodA) (15). Given the facts that (*i*) *Bb* does not accumulate iron (23)

MICROBIOLOGY

Table 1. Infectivity of *B. burgdorferi* clones in mice

Strain, clone	Description	Dose	No. of cultures positive/total no. of specimens examined				No. of mice infected/ total no. of mice
			Heart	Joint	Skin	All sites	
297	WT B. burgdorferi	10^4	7/7	7/7	7/7	21/21	7/7
OY04/D4	297, ΔbmtA*	10^4	0/6	0/6	0/6	0/18	0/6
OY04/F42	297, ΔbmtA	10^4	0/6	0/6	0/6	0/18	0/6
OY04/D4	297, ΔbmtA	10^7	0/5	0/5	0/5	0/15	0/5
OY04/F42	297, ΔbmtA	10^7	0/5	0/5	0/5	0/15	0/5
OY06/F6	OY04/D4 transformed with pOY15	10^4	3/3	3/3	3/3	9/9	3/3
OY06/D11	OY04/F42 transformed with pOY15	10^4	3/3	3/3	3/3	9/9	3/3
OY07/F1	OY04/D4 transformed with pJD54	10^4	0/3	0/3	0/3	0/9	0/3
OY07/F62	OY04/F42 transformed with pJD54	10^4	0/3	0/3	0/3	0/9	0/3
OY07/F1	OY04/D4 transformed with pJD54	10^7	0/3	0/3	0/3	0/9	0/3
OY07/F62	OY04/F42 transformed with pJD54	10^7	0/3	0/3	0/3	0/9	0/3

*Δ*bmtA*: *bmtA* mutant.

but does accumulate Mn (Mn accumulation was severely impaired in the *bmtA* mutant), (*ii*) Mn is believed to be involved in the oxidative stress response of a number of pathogens (17, 31, 32), and (*iii*) *Bb* SodA (BB0153) has been predicted to be Mn-dependent (22, 33), we explored whether the inactivation of *bmtA* adversely impacted *Bb*'s ability to detoxify intracellular superoxide. When WT 297 was exposed to 5 mM or 10 mM *t*-butyl hydroperoxide, ≈100% or 93%, respectively, of the cells survived (Fig. 5). In contrast, the *bmtA* mutant was significantly more sensitive to *t*-butyl hydroperoxide, with a survival of ≈50% at 5 mM *t*-butyl hydroperoxide. These data suggest that BmtA and Mn play important roles in the detoxification of ROS (i.e., oxidative stress response).

Discussion

Analyses of genomic sequence information have suggested that the utilization of transition metals by *Bb* may be dramatically different from other bacteria. For example, in contrast to most bacterial pathogens, *Bb* does not appear to require iron to support its growth (23). Rather, it was reported that *Bb* accumulated Mn when grown in a serum-free medium (23), but the relevance of this finding to what occurs when *Bb* is cultivated in more nutrient-rich (e.g., serum-containing) environments, or what *Bb* encounters in ticks or mammalian hosts, has remained obscure. It additionally has been unknown to what extent Mn may be important for establishing mammalian infection by *Bb*.

Employing molecular genetics to create BmtA mutants and complemented strains, here we have identified what appears to be a novel Mn transporter in *Bb*. We derived this conclusion from 2 key observations. First, BmtA has a predicted topology similar to Zn transporters (ZIP proteins) (25); in our analyses, BmtA was predicted to be a cytoplasmic membrane protein containing 8 transmembrane domains (26, 28). Second, our data clearly showed that BmtA is critical for Mn uptake in *Bb*, at least when *Bb* is grown in BSK medium. Therefore, it is likely that *bmtA* encodes a transporter mediating the uptake of Mn across the cytoplasmic membrane of *Bb*.

Our study is significant in at least two major ways. First, to our knowledge, no metal transporter had thus far been reported in this important human pathogen. Second, 3 classes of Mn transporters have been characterized in prokaryotes, including the natural resistance-associated macrophage protein (Nramp) type Mn transporter, the ATP-binding cassette (ABC) Mn permease, and the P-type ATPase Mn transporter (15, 17, 34). Sequence

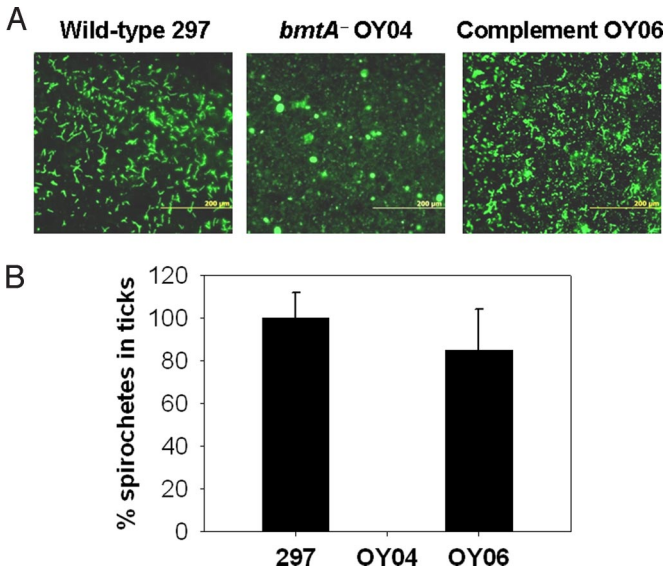

Fig. 4. BmtA is required by *Bb* to infect and survive in ticks. Unfed *I. scapularis* nymphs were microinjected with various *Bb* strains and were allowed to feed to repletion on normal mice. After detachment, fed nymphs were dissected, and the tick tissue contents were subjected to immunofluorescence assays with FITC-labeled anti-*Bb* antibody. (*A*) Confocal immunofluorescence microscopy; spirochete morphology is evident from tissues of ticks infected with WT 297 or the complemented (OY06) strains. (*B*) Quantitative assessment (number of borreliae per microscope field) of the data shown in *A*; WT 297 was considered the 100% value.

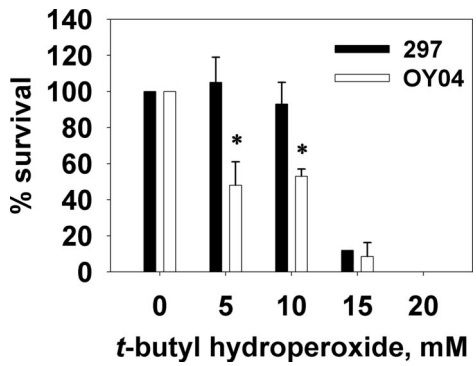

Fig. 5. The *bmtA* mutant is sensitive to treatment with *t*-butyl hydroperoxide. *Bb* (WT 297 or *bmtA* mutant OY04/D4) was grown to a cell density of 1×10^7 cells/mL and then treated with varying amounts of *t*-butyl hydroperoxide. Averages with standard deviations are shown. The asterisk denotes a significant difference in *t*-butyl hydroperoxide sensitivity ($P < 0.05$).

similarity searching revealed that BmtA has no homology to any of these bacterial Mn transporters. Despite this, we found that the ZIP domain-carrying BmtA protein is involved in the transport of Mn but not Zn. This is particularly striking, given that ZIP domains typically are involved in Zn transport (25). Our study thus not only provides further insights into the physiological functions of bacterial ZIP proteins, but also suggests that BmtA and its homologs comprise a novel mechanism(s) for Mn acquisition.

Because of their similar ionic radius and chelate structures, Mn^{2+}, Fe^{2+}, Mg^{2+}, and Zn^{2+} are interchangeable in the metal-binding site of many proteins. In this regard, Mn in place of iron has been proposed to be required by *Bb* (23). Unlike most pathogens that possess overlapping or redundant Mn transporters, *Bb* probably expresses only one Mn transporter, BmtA, at least when borreliae are grown in vitro. This contention is strongly supported by our data that Mn was not detected in the BmtA mutant. Regarding the fact that the mutant had no substantial growth defect in vitro or in DMCs, we propose that Mn is not an obligate requirement for *Bb* physiology, although it may facilitate optimal growth of borreliae in vitro. Because Zn may substitute for activities typically served by Fe or Mn, when Mn is not available in the environment, *Bb* may switch its requirement from Mn to Zn. Consistent with this assertion, our data showed that the *bmtA* mutant accumulated more Zn than the WT strain, ostensibly through the activation of one or more potential Zn transporter(s). Transcriptional profiling comparisons between WT, *bmtA* mutants, and complemented strains might shed added light on this possibility. Alternatively, in addition to the import of Mn, BmtA may also be involved in the efflux of Zn, in so much that this dual import–export function has been noted for other bacterial metal transporters (e.g., CorA) (35). Finally, it remains possible that the physiological functions of Mn also may be served by Mg because of their similar structure.

Inactivation of *bmtA* rendered *Bb* completely noninfectious for mice and unable to infect and proliferate in ticks, indicating that BmtA is essential for *Bb*'s mammalian infectivity and colonization of its arthropod vector, even though BmtA and Mn are dispensable when *Bb* is cultivated in vitro. The contribution of Mn transporters and Mn to bacterial pathogenesis has been well established in many other pathogens, including in those where Mn is not an obligate requirement for bacterial growth in vitro (15, 17, 31). Mn typically is not a widely used cofactor in biology and serves as a physiological cofactor for only a handful of enzymes (15, 17). Therefore, if Mn is dispensable when bacteria are cultivated in vitro, why is it important for bacterial virulence? In the case of *Bb*, one possibility is that BSK medium does not recapitulate the physiological or metal conditions that *Bb* encounters in either ticks or mammals. However, there are a number of additional observations in our study that may address this question. First, in comparison with WT, the *Bb bmtA* mutant was sensitive to *t*-butyl hydroperoxide, suggesting that BmtA (and thus Mn) is probably involved in the detoxification of ROS. Akin to the situation for other bacterial pathogens (17, 31, 32), the most obvious role for BmtA and Mn likely is in the *Bb* oxidative stress response. For example, in the process of tick feeding or during the process of mammalian host dissemination, BmtA and Mn may be required by *Bb* to counter superoxide contained in mammalian blood (36, 37). Further, BmtA and Mn may also play a role in defending the spirochete from the initial host immune response, including the extremely deleterious effects of ROS generated during the innate host immune response to Lyme borreliosis (36). Although entirely speculative, borrelial Mn-dependent SodA also may participate in one or more of these events. Finally, in a wide variety of bacterial pathogens, Mn contributes to virulence by regulating the expression of many virulence determinants (15, 17, 31). Similarly, Mn, possibly via the Mn-dependent Fur homolog BosR (23, 33, 37, 38), might play a critical role in controlling *Bb* virulence. Future microarray studies may shed additional light on to what extent BmtA, and by inference Mn, regulates virulence expression in *Bb*.

Our study has demonstrated that the Lyme disease spirochete requires BmtA's Mn-associated transport function(s) to maintain its infectious cycle in nature. To date, only relatively few virulence factors, including OspC, DbpB/A, OspA/B, PncA, and BptA, have been identified in *Bb*, and the functions of most of these proteins remain obscure (4, 5, 7–10). In this regard, our identification of BmtA as a novel virulence factor in *Bb* provides further insights into molecular mechanisms that contribute to *Bb*'s survival in nature and may lead to new strategies to interrupt the spirochete life cycle. In addition, our findings represent a first step in elucidating transition metal homeostasis in *Bb*. Our study also prompts a number of salient questions. First, considering the predicted topology of BmtA, we propose that the theoretical 8 transmembrane segments assemble a channel to allow Mn or other ions to pass through the cytoplasmic membrane. However, how the channel is opened or closed, how the metal ions are transported, or whether energy is required remain completely unknown. It also is unknown whether BmtA is involved in the transport of other cations, as the affinities and selectivity of BmtA for Mn and other cations have not yet been fully assessed. Biochemical experiments with recombinant BmtA and, possibly, reconstitution into liposomes may be strategic for addressing some of these questions. Second, what are the functional relationships between the other 5 members of the *bmtA* operon? Although none of these 5 proteins was predicted to be implicated in metal transport, it remains possible that they indeed contribute to Mn transport. Inactivation of each gene of the operon may shed additional light on this issue. Finally, what are the specific cellular processes in *Bb* for which Mn is required? In many pathogens, Mn transport is controlled by an Mn-specific transcription factor, MntR, as well as by Fur, PerR, or OxyR (15, 17, 31). Although BosR in *Bb* was predicted to be Mn-dependent (23), it is not clear whether *bmtA* is regulated by BosR or responses to the intracellular Mn pool. Examination of *bmtA* transcriptional control using reporter assays may help to clarify the regulation of *bmtA*.

Methods

Bacterial Strains and Culture Conditions. Infectious *Bb* strain 297 (39) was used as the WT strain throughout this study. *Bb* was cultured at 37 °C in BSK-II medium (40) supplemented with 6% rabbit serum (Pel-Freeze). To assess the growth of *Bb* in a mammalian host-adapted state, borreliae were also cultivated within DMCs implanted into the peritoneal cavities of rats, as previously described (41). All animal experiments were approved by the Institutional Animal Care and Use Committee at UT Southwestern Medical Center (Dallas, TX).

Construction of *bmtA* Mutants and Complemented Strains. The *bmtA* mutant strain OY04 was created by allelic exchange in *Bb* 297 using a suicide vector pOY04. The mutation in *bmtA* was complemented by transforming a shuttle vector, pOY15, based on the pJD54 plasmid, into the *bmtA* mutant, generating OY06. In addition, a mock-complemented mutant, OY07, was constructed by transforming pJD54 into *Bb* OY04. All plasmid constructs were characterized by PCR, restriction digestion, and sequence analysis (*SI Methods*). Transformation of *Bb* was performed as previously described (12, 14). Plasmid contents of all *Bb* strains were determined by PCR using specific primers (4).

Intracellular Metal Contents. Intracellular metal contents of borreliae were measured as previously described (19). Briefly, bacterial cultures grown to stationary phase were harvested, and the pellets were lysed by using 65% HNO_3 (TraceMetal grade; Sigma). The metal contents in the lysates were measured by using inductively coupled plasma atomic emission spectrometry by the Research Analytical Laboratory, University of Minnesota (St. Paul, MN;

SI Methods). Three independent tests were performed, and the results were analyzed by using Student's *t* test.

Sensitivity of *Bb* to ROS. This test was performed as previously described, with modifications (36, 37). Briefly, when spirochete growth reached a cell density of 5×10^7 cells/mL, the culture was divided into 5 aliquots and treated with varying concentrations of oxidants (0–20 mM *t*-butyl hydroperoxide) at 37 °C for 4 h. After incubation, cells were serially diluted in fresh BSK medium in a 96-well plate and incubated for 2 weeks. Percent survivability was calculated as the number of clones recovered from the treated group versus the number of clones recovered from the untreated group.

***Bb* Infection of Mice.** The infectivity of *Bb* clones was assessed by using the murine needle-challenge model of Lyme borreliosis (42). C3H/HeN mice (Charles River Laboratories) were infected via intradermal injection with various concentrations of *Bb*. At 4 weeks after inoculation, skin, heart, and joint tissues were collected and cultured in BSK supplemented with 1× *Borrelia* antibiotic mixture (Sigma). The outgrowth of spirochetes in these cultures was assessed by using darkfield microscopy.

Artificial Infection of Ticks with *Bb*. *I. scapularis* nymphs or larvae (obtained from the Tick Rearing Facility at Oklahoma State University, Stillwater, OK) were artificially infected with various strains of *Bb* by using a microinjection technique (11, 43) or an immersion method (30) (see *SI Methods*). After infection, ticks were fed to repletion on separate naïve C3H/HeN mice. Subsets of ticks were dissected immediately and analyzed by immunofluoresence assay (*SI Methods*). Spirochetes were stained with the BacTrace FITC-conjugated goat anti-*Bb* antibody (Kirkegaard and Perry Laboratories) and observed by using an Olympus BX50 fluorescence microscope.

ACKNOWLEDGMENTS. We thank Farol Tomson and Eric Hansen for critical reading of the manuscript. This work was supported by National Institutes of Health Public Health Service Grant AI-059062 from the National Institute of Allergy and Infectious Diseases.

1. CDC (2007) Lyme disease–United States, 2003–2005. *MMWR Morb Mortal Wkly Rep* 56:573–576.
2. Burgdorfer W, *et al.* (1982) Lyme disease-a tick-borne spirochetosis? *Science* 216:1317–1319.
3. Steere AC, *et al.* (1983) The spirochetal etiology of Lyme disease. *N Engl J Med* 308:733–740.
4. Blevins JS, Hagman KE, Norgard MV (2008) Assessment of decorin-binding protein A to the infectivity of *Borrelia burgdorferi* in the murine models of needle and tick infection. *BMC Microbiol* 8:82.
5. Grimm D, *et al.* (2004) Outer-surface protein C of the Lyme disease spirochete: A protein induced in ticks for infection of mammals. *Proc Natl Acad Sci USA* 101:3142–3147.
6. Neelakanta G, *et al.* (2007) Outer surface protein B is critical for *Borrelia burgdorferi* adherence and survival within *Ixodes* ticks. *PLoS Pathog* 3:e33.
7. Purser JE, *et al.* (2003) A plasmid-encoded nicotinamidase (PncA) is essential for infectivity of *Borrelia burgdorferi* in a mammalian host. *Mol Microbiol* 48:753–764.
8. Revel AT, *et al.* (2005) *bptA* (*bbe16*) is essential for the persistence of the Lyme disease spirochete, *Borrelia burgdorferi*, in its natural tick vector *Proc Natl Acad Sci USA* 102:6972–6977.
9. Shi Y, Xu Q, McShan K, Liang FT (2008) Both decorin-binding proteins A and B are critical for overall virulence of *Borrelia burgdorferi. Infect Immun* 76:1239–1246.
10. Yang XF, Pal U, Alani SM, Fikrig E, Norgard MV (2004) Essential role for OspA/B in the life cycle of the Lyme disease spirochete. *J Exp Med* 199:641–648.
11. Boardman BK, *et al.* (2008) Essential role of the response regulator Rrp2 in the infectious cycle of *Borrelia burgdorferi. Infect Immun* 76:3844–3853.
12. Hubner A, *et al.* (2001) Expression of *Borrelia burgdorferi* OspC and DbpA is controlled by a RpoN-RpoS regulatory pathway. *Proc Natl Acad Sci USA* 98:12724–12729.
13. Ouyang Z, Blevins JS, Norgard MV (2008) Transcriptional interplay among the regulators Rrp2, RpoN and RpoS in *Borrelia burgdorferi. Microbiology* 154:2641–2658.
14. Yang XF, Alani SM, Norgard MV (2003) The response regulator Rrp2 is essential for the expression of major membrane lipoproteins in *Borrelia burgdorferi. Proc Natl Acad Sci USA* 100:11001–11006.
15. Jakubovics NS, Jenkinson HF (2001) Out of the iron age: New insights into the critical role of manganese homeostasis in bacteria. *Microbiology* 147:1709–1718.
16. Hantke K (2001) Bacterial zinc transporters and regulators. *Biometals* 14:239–249.
17. Papp-Wallace KM, Maguire ME (2006) Manganese transport and the role of manganese in virulence. *Annu Rev Microbiol* 60:187–209.
18. Wandersman C, Delepelaire P (2004) Bacterial iron sources: From siderophores to hemophores. *Annu Rev Microbiol* 58:611–647.
19. Ouyang Z, Isaacson R (2006) Identification and characterization of a novel ABC iron transport system, *fit*, in *Escherichia coli. Infect Immun* 74:6949–6956.
20. Patzer SI, Hantke K (2001) Dual repression by Fe^{2+}-Fur and Mn^{2+}-MntR of the *mntH* gene, encoding an NRAMP-like Mn^{2+} transporter in *Escherichia coli. J Bacteriol* 183:4806–4813.
21. Grass G, Wong MD, Rosen BP, Smith RL, Rensing C (2002) ZupT is a Zn(II) uptake system in *Escherichia coli. J Bacteriol* 184:864–866.
22. Fraser CM, *et al.* (1997) Genomic sequence of a Lyme disease spirochaete, *Borrelia burgdorferi. Nature* 390:580–586.
23. Posey JE, Gherardini FC (2000) Lack of a role for iron in the Lyme disease pathogen. *Science* 288:1651–1653.
24. Eng BH, Guerinot ML, Eide D, Saier MH Jr. (1998) Sequence analyses and phylogenetic characterization of the ZIP family of metal ion transport proteins. *J Membr Biol* 166:1–7.
25. Guerinot ML (2000) The ZIP family of metal transporters. *Biochim Biophys Acta* 1465:190–198.
26. Krogh A, Larsson B, von Heijne G, Sonnhammer EL (2001) Predicting transmembrane protein topology with a hidden Markov model: Application to complete genomes. *J Mol Biol* 305:567–580.
27. McGowan SJ, Gorham HC, Hodgson DA (1993) Light-induced carotenogenesis in *Myxococcus xanthus*: DNA sequence analysis of the *carR* region. *Mol Microbiol* 10:713–735.
28. Gardy JL, *et al.* (2005) PSORTb v. 2.0: Expanded prediction of bacterial protein subcellular localization and insights gained from comparative proteome analysis. *Bioinformatics* 21:617–623.
29. Rosa PA, Tilly K, Stewart PE (2005) The burgeoning molecular genetics of the Lyme disease spirochaete. *Nat Rev* 3:129–143.
30. Policastro PF, Schwan TG (2003) Experimental infection of *Ixodes scapularis* larvae (Acari: *Ixodidae*) by immersion in low passage cultures of *Borrelia burgdorferi. J Med Entomol* 40:364–370.
31. Horsburgh MJ, *et al.* (2002) MntR modulates expression of the PerR regulon and superoxide resistance in *Staphylococcus aureus* through control of manganese uptake. *Mol Microbiol* 44:1269–1286.
32. Wu HJ, *et al.* (2006) PerR controls Mn-dependent resistance to oxidative stress in *Neisseria gonorrhoeae. Mol Microbiol* 60:401–416.
33. Boylan JA, Posey JE, Gherardini FC (2003) *Borrelia* oxidative stress response regulator, BosR: A distinctive Zn-dependent transcriptional activator. *Proc Natl Acad Sci USA* 100:11684–11689.
34. Archibald F (1986) Manganese: Its acquisition by and function in the lactic acid bacteria. *Crit Rev Microbiol* 13:63–109.
35. Lunin VV, *et al.* (2006) Crystal structure of the CorA Mg^{2+} transporter. *Nature* 440:833–837.
36. Boylan JA, Lawrence KA, Downey JS, Gherardini FC (2008) Borrelia burgdorferi membranes are the primary targets of reactive oxygen species. *Mol Microbiol* 68:786–799.
37. Seshu J, *et al.* (2004) A conservative amino acid change alters the function of BosR, the redox regulator of *Borrelia burgdorferi. Mol Microbiol* 54:1352–1363.
38. Katona LI, Tokarz R, Kuhlow CJ, Benach J, Benach JL (2004) The *fur* homologue in *Borrelia burgdorferi. J Bacteriol* 186:6443–6456.
39. Hughes CA, Kodner CB, Johnson RC (1992) DNA analysis of *Borrelia burgdorferi* NCH-1, the first northcentral U.S. human Lyme disease isolate. *J Clin Microbiol* 30:698–703.
40. Pollack RJ, Telford SR, III, Spielman A (1993) Standardization of medium for culturing Lyme disease spirochetes. *J Clin Microbiol* 31:1251–1255.
41. Akins DR, Bourell KW, Caimano MJ, Norgard MV, Radolf JD (1998) A new animal model for studying Lyme disease spirochetes in a mammalian host-adapted state. *J Clin Invest* 101:2240–2250.
42. Barthold SW, de Souza MS, Janotka JL, Smith AL, Persing DH (1993) Chronic Lyme borreliosis in the laboratory mouse. *Am J Pathol* 143:959–971.
43. Narasimhan S, *et al.* (2004) Disruption of *Ixodes scapularis* anticoagulation by using RNA interference. *Proc Natl Acad Sci USA* 101:1141–1146.